Am J Physiol Renal Physiol 297: F155–F162, 2009.
First published May 6, 2009; doi:10.1152/ajprenal.00114.2009.

Detection of low-frequency oscillations in renal blood flow

K. L. Siu,[1] B. Sung,[2] W. A. Cupples,[3] L. C. Moore,[2] and K. H. Chon[1]

Departments of [1]Biomedical Engineering and [2]Physiology and Biophysics, SUNY Stony Brook, Stony Brook, New York; and [3]Department of Biology, University of Victoria, Victoria, British Columbia, Canada

Submitted 26 February 2009; accepted in final form 3 May 2009

Siu KL, Sung B, Cupples WA, Moore LC, Chon KH. Detection of low-frequency oscillations in renal blood flow. *Am J Physiol Renal Physiol* 297: F155–F162, 2009. First published May 6, 2009; doi:10.1152/ajprenal.00114.2009.—Detection of the low-frequency (LF; ~0.01 Hz) component of renal blood flow, which is theorized to reflect the action of a third renal autoregulatory mechanism, has been difficult due to its slow dynamics. In this work, we used three different experimental approaches to detect the presence of the LF component of renal autoregulation using normotensive and spontaneously hypertensive rats (SHR), both anesthetized and unanesthetized. The first experimental approach utilized a blood pressure forcing in the form of a chirp, an oscillating perturbation with linearly increasing frequency, to elicit responses from the LF autoregulatory component in anesthetized normotensive rats. The second experimental approach involved collection and analysis of spontaneous blood flow fluctuation data from anesthetized normotensive rats and SHR to search for evidence of the LF component in the form of either amplitude or frequency modulation of the myogenic and tubuloglomerular feedback mechanisms. The third experiment used telemetric recordings of arterial pressure and renal blood flow from normotensive rats and SHR for the same purpose. Our transfer function analysis of chirp signal data yielded a resonant peak centered at 0.01 Hz that is greater than 0 dB, with the transfer function gain attenuated to lower than 0 dB at lower frequencies, which is a hallmark of autoregulation. Analysis of the data from the second experiments detected the presence of ~0.01-Hz oscillations only with isoflurane, albeit at a weaker strength compared with telemetric recordings. With the third experimental approach, the strength of the LF component was significantly weaker in the SHR than in the normotensive rats. In summary, our detection via the amplitude modulation approach of interactions between the LF component and both tubuloglomerular feedback and the myogenic mechanism, with the LF component having an identical frequency to that of the resonant gain peak, provides evidence that 0.01-Hz oscillations may represent the third autoregulatory mechanism.

spontaneously hypertensive rats; renal autoregulation; myogenic; TGF; amplitude modulation; frequency modulation

THE LONG-TERM REGULATION OF systemic blood pressure (BP) is one of the major functions of the kidney. The functional unit of the kidney, the nephron, requires a stable input of fluid to perform its function. However, systemic BP fluctuates over a large range of frequencies, which would destabilize renal function without a proper control mechanism to compensate for blood flow variations (11). It is known that the nephron has the ability to regulate its own blood flow, a phenomenon termed autoregulation. Another role of the autoregulatory mechanism is to provide protection for the renal vasculature from large fluctuations in systemic pressure (1, 2). Abnormalities in the autoregulatory mechanisms have been implicated in many diseases, such as hypertension-induced renal disease and chronic renal failure (1, 2).

Renal autoregulation is widely accepted to be mediated by two mechanisms. The first is the slower of the two mechanisms, the tubuloglomerular feedback mechanism (TGF), which oscillates between 0.02 and 0.05 Hz in rats (9, 10). The myogenic mechanism (MYO) is faster than TGF and exhibits oscillations in the frequency range between 0.1 and 0.3 Hz (13, 30). On the basis of experiments using a step decrease in BP, Just et al. (12, 14) have proposed the existence of a slower, third autoregulatory mechanism which operates at ~0.01 Hz. To date, little is known about its mechanistic origin, but its operating time scale may indicate involvement of ANG II (23). The presence of the third mechanism is somewhat controversial because assessments of autoregulation dynamics using broad-band BP perturbations have not revealed such a low-frequency (LF) component (16, 17). However, there are two possible reasons behaviors consistent with the third mechanism have not been observed in these dynamic autoregulation studies. First, preprocessing of renal BP and blood flow data often involves detrending, which may well have filtered out any ~0.01-Hz oscillation. Second, the time interval and, hence, the number of data points analyzed are limited when traditional power spectral methods are used, and this makes it difficult to detect LF peaks.

One computational approach to discern the presence of the autoregulatory mechanisms is to look for their interactions. An example is an elegant study by Schnermann and Briggs (21) which demonstrated that the strength of the TGF response depends on the state of the MYO system at the single-nephron level. Furthermore, evidence of interactions between the two autoregulatory mechanisms was buttressed by a study in which Chen et al. (3) showed that coupling exists between nephrons that have physiological vascular connections. Consequently, such interaction phenomena were detected in both single nephrons and whole kidneys using a myriad of computational approaches, including the Volterra-Wiener kernel (5), the bispectrum (22), frequency and amplitude modulation (25, 26), and frequency locking via a wavelet method (27).

In this work, we utilized three separate experimental approaches to detect the LF oscillation, which is thought to be related to a third autoregulatory mechanism. In the first experimental approach, we used a chirp signal forcing in the BP of anesthetized normotensive rats to elicit characteristic oscillations associated with the LF component. Given the fact that both TGF and MYO interact, and if the putative third mechanism does indeed exist, it is reasonable to assume that it should also be coupled to the two other autoregulatory mechanisms. Thus, in the second and third experimental approaches, we hypothesize that the putative third autoregulatory mechanism interacts with the MYO and TGF mechanisms and that the interactions should be evident in the spontaneous blood flow fluctuation data. The computational method we used in this study, complex demodulation (CDM), provides very high res-

Address for reprint requests and other correspondence: K. H. Chon, Dept of Biomedical Engineering, SUNY Stony Brook, HSC T18, Rm. 030, Stony Brook, NY 11794-8181 (e-mail: ki.chon@sunysb.edu).

olution of time-frequency spectra, which is required to resolve the LF oscillations associated with the operation of the third mechanism (12, 14). Specifically, we used CDM to identify either amplitude modulation (AM) or frequency modulation (FM) in the frequency bands normally associated with the TGF and MYO mechanisms, since they would be the result of any interaction phenomenon. Thus the aim of the study is to verify the presence of the third autoregulatory mechanism by looking for its interactions with the MYO and TGF mechanisms and to determine whether the transfer function gain magnitude from the chirp signal experiment provides the signature of the dynamics of autoregulation.

METHODS

Animal Preparation

Experiment 1, as described below, was performed for the present study in the laboratory of Dr. W. A. Cupples. *Experiments 2* and *3* below were performed for the present study in the laboratory of Dr. K. H. Chon.

Experiment 1: chirp signal BP perturbation. The first experiment was approved by the Animal Care Committee of the University of Victoria and was conducted under the guidelines promulgated by the Canadian Council on Animal Care. Five adult male Long-Evans rats (~300 g) had free access to water and food at all times before the acute experiments. These animals are normotensive, and we have shown previously that their renal blood flow dynamics are remarkably similar to those of other normotensive strains (29). Twenty minutes before anesthesia, each rat received buprenorphine (Temgesic, 0.01 mg/kg ip, Reckitt and Colman Pharmaceuticals, Wayne, NJ). Anesthesia was induced by 5% isoflurane in inspired gas (30% O_2-70% air). After induction, the anesthetic concentration was reduced ~2%. The animal was transferred to a servo-controlled heated table to maintain body temperature at 37°C, intubated, and ventilated by a respirator (RSP 1002, Kent Scientific, Litchfield, CT). During the 1-h postsurgical equilibration period, inspired anesthetic concentration was titrated to the minimum concentration that precluded a BP response when the tail was pinched (~1%).

Cannulas were placed in the right femoral artery and vein. A constant infusion delivered 1% of body weight per hour throughout the experiment and contained 2% charcoal-washed bovine serum albumin in normal saline. The left kidney was approached by a flank incision, immobilized in a plastic cup, and covered with plastic wrap. The flow probe (1PRB, driven by a Transonic Systems model T401 flowmeter, Transonic Systems, Ithaca, NY) was placed around the renal artery; it was fixed in place and the acoustic coupling was ensured as recommended by the manufacturer. Femoral arterial pressure was measured by a Kent pressure transducer (TRN050) driven by a TRN005 amplifier.

A motorized clamp was placed on the aorta between the right and left renal arteries and was used to force BP. The motor was driven by a program which operates in a negative-feedback manner to impose chirp forcing of renal perfusion pressure 15–20% below the spontaneous level of BP. Care was taken to ensure that renal perfusion pressure remained within the autoregulatory range at all times. Data were low-pass filtered at 40 Hz and digitized with 12-bit resolution at 200 Hz.

Experiment 2: AM and FM detection in anesthetized animals. For the acute experiments, 24 animals [6 Sprague-Dawley rats (SDR) and 6 spontaneously hypertensive rats (SHR) for each anesthetic] were anesthetized with either inactin (135 mg/kg) or isoflurane (3% initial, 1% maintenance). The animals were then placed on a servo-controlled heated table to maintain a body temperature of 37°C. A tracheostomy was performed to aid respiration. The right femoral artery and vein were catheterized (PE-50 and PE-10, respectively) for BP measurement and infusion of isotonic saline to compensate for surgical fluid losses, respectively. The left kidney was isolated and placed in a Lucite cup. An ultrasonic flow probe (series 1PR, Transonic Systems) was placed around the renal artery for measurement of renal blood flow. The animals were allowed 1 h to recover from surgical stress before experimental measurements were made.

Experiment 3: AM and FM detection via telemetric measurement. Male SDR and SHR, weighing between 200 and 250 g (Taconic Farms), were used in the experiments. All experimental protocols were approved by the institutional guidelines of animal care and use in research and approved by the Institutional Research Board (IACUC no. 20081267) on the use of animals for research at the State University of New York at Stony Brook. Before surgery, the animals had free access to standard rat chow and tap water and were housed individually in a temperature-controlled room with a 12:12-h light-dark cycle. A total of five SDRs and five SHRs were used.

Animals were anesthetized using pentobarbital sodium (50 mg/kg ip). After induction of anesthesia, an ultrasonic flow probe (series 1PR, Transonic Systems) was placed around the left renal artery. The cannula of a BP telemeter (PA-C40, Data Sciences International, St. Paul, MN) was also implanted into the right femoral artery. After surgery, the animal was placed on a heated pad to facilitate recovery from anesthesia. The animals were studied after a 1-wk period of surgical recovery. Animals were monitored for signs of infection on a daily basis.

Experimental Protocol

For the telemetric experiment, each animal was housed individually in a temperature-controlled room set on a 12:12-h light-dark cycle with free access to standard rat chow and tap water. After the connection of the animal to the blood flow-recording equipment, the animal was allowed a 15-min adjustment period before measurements began. Renal blood flow (RBF) and systemic BP were measured for 2 h each day starting at 10 AM for a period of 1 wk. During the recording period, spontaneous activity of the animal was recorded by the investigator. Only data segments collected when the animal was at rest were analyzed to avoid movement artifacts. For the acute experiments, performed under anesthesia, spontaneous BP and RBF were recorded for 1 h after the recovery period.

For the telemetric experiment, data were recorded at a sampling rate of 250 Hz using the Dataquest A.R.T. system (Data Sciences International, St. Paul, MN). For the acute experiment, data were collected at 100 Hz using a Powerlab 16RSP analog-to-digital converter (ADInstruments, Colorado Springs, CO). All data were down-sampled to 1-Hz sampling rate following digital low-pass filtering to avoid aliasing.

Chirp BP Forcing

The LF response characteristics of blood flow fluctuations in anesthetized Long-Evans rats were investigated by imposing a sinusoidal forcing with linearly increasing frequency (0.001–0.02 Hz) on renal perfusion pressure. The rationale for using a chirp signal on the BP forcing is to excite any autoregulation mechanism that may resonate within the perturbation frequency band. While we were primarily interested in detecting 0.01-Hz oscillations, we used a wide range of frequencies (0.001–0.02 Hz) for the BP forcing to avoid introducing bias and to indentify other possible oscillations.

A flowchart of the data processing steps along with a representative data set are shown in Fig. 1. The first row shows the chirp signal of the BP forcing and the resultant RBF data. The first step is to calculate the time-frequency spectrum of each signal using a CDM approach, as shown in the second row. Note the linearly increasing frequency in BP perturbation and RBF response. Next, the magnitude of the peak frequency was tracked across time, as shown in the third row. Finally, the ratio between the RBF and the BP spectral amplitudes across time was calculated, as shown in the fourth row, plotted in log scale. Ratio values above the threshold of 0, shown as the dotted line, indicate characteristic resonance of the autoregulation system. Note that since the frequency increases linearly with time, the *x*-axis in this figure can also be plotted in terms of frequency.

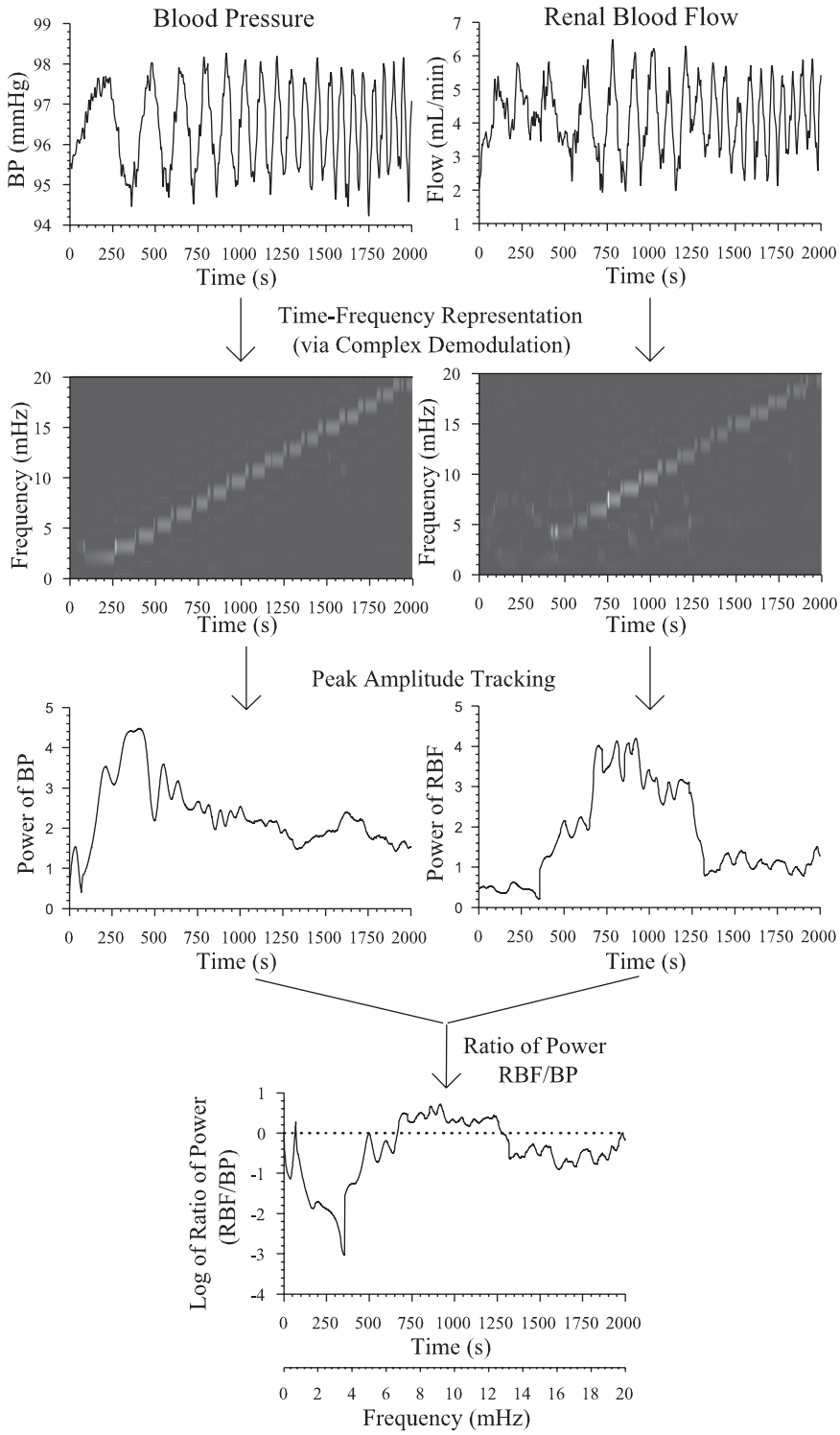

Fig. 1. Flowchart showing the data analysis procedures used for the chirp forcing experiment ($n = 5$). The *top* row shows the representative blood flow data. The *middle* row shows the time-varying spectra calculated via the complex demodulation method. The *bottom* row shows time traces of the peak amplitude across time for each spectrum. The *bottom* panel shows the ratio between the 2 amplitude tracking time traces; the dotted line shows the threshold of 0, where ratios >0 indicate the presence of a resonant component. BP, blood pressure; RBF, renal blood flow.

AM and FM Detection Algorithms

AM and FM denote that either the amplitude or the frequency of a component in a signal, termed the carrier signal, is changed by another oscillatory mode, termed the modulation signal

$$m(t) = M \cdot \cos(\omega_m t + \theta_m)$$

where M is the modulation magnitude, and ω_m and θ_m are the modulation frequency and phase, respectively. The unmodulated carrier signal is denoted as

$$c(t) = C \cdot \cos(\omega_c t + \theta_c)$$

where C is the carrier magnitude, and ω_c and θ_c are the carrier frequency and phase, respectively. For AM, the amplitude of the carrier signal is modulated, such that

$$c_{modulated}(t) = [C + m(t)] \cdot \cos(\omega_c t + \theta_c)$$

For FM, the modulating frequency is calculated by an integral, such that

$$C_{\text{modulated}} = C \cdot \cos\left(2\pi f_c t + \int_0^t m(\tau)d\tau\right)$$

Simulated data containing AM were created to illustrate the concepts. In this simulation, components with frequencies to those exhibited by renal autoregulatory mechanisms were used. Specifically, two carrier frequencies, at 0.03 and 0.12 Hz, were modulated by a 0.01-Hz mechanism. Figure 2, *A* and *B*, shows AM signals. Figure 2*A* shows the higher carrier frequency (0.12 Hz) modulated by 0.01 Hz, while Fig. 2*B* shows the lower carrier frequency (0.03 Hz) modulated by 0.01 Hz. Figure 2*C* shows the composite signal that combines both the high and low frequency signals in panels *A* and *B*.

The general approach to detecting AM is shown in Fig. 2, *D–H*. The first step is to calculate the time-frequency representation (TFR) of the original signal using CDM (Fig. 2*D*). The CDM was chosen for this calculation as it has been shown to have one of the highest frequency and time resolutions while preserving accurate amplitude information (28). After the calculation of the TFR, the average amplitudes at the MYO and TGF frequency bands were extracted (0.1–0.3 and 0.02–0.05 Hz, respectively), as shown in Fig, 2, *E* and *F*. Next, the frequency spectra of these extracted time traces were calculated to show the frequency and magnitude of modulation, shown as the solid line in Fig. 2, *G* and *H*. For illustration purposes, the maximum magnitude of these spectra is shown to be 1. For this algorithm, only modulation at the low-frequency range (0–0.02 Hz) was examined. The reason for this is to avoid detecting TGF modulation when the method is used with actual blood flow renal data. Note that the peak of this spectrum is correctly shown to be at a simulated modulation frequency of 0.01 Hz. This simulation illustrates how even a LF component (~0.01 Hz) can be reliably detected by looking for AM phenomena with the aid of a high-resolution time-frequency spectral method.

For FM detection, we employed a weighted average method to account for varying MYO frequencies in the 0.1- to 0.3-Hz band. Specifically, for each time point, any spectral peak that is above Gaussian white noise (GWN)-derived threshold values (as detailed in the proceeding paragraph) is selected. A weighted average frequency was calculated by summing the frequency of all significant peaks multiplied by their own individual magnitude. This sum was then divided by the sum of the magnitudes of the significant peaks (e.g., $\overline{f_w} = \frac{\sum_{i=1}^{N}(f_i A_i)}{\sum_{i=1}^{N} A_i}$). In essence, this calculation provides a weighted frequency average based on the strength of each frequency peak.

To assess the significance of this modulation, a statistical threshold based on GWN was calculated; it is shown as the dotted line in Fig 2, *G* and *H*. To obtain this threshold, 1,000 realizations of GWN with the same data length and variance as the original data signal were generated. Each realization of GWN was analyzed with the modulation detection algorithm, resulting in 1,000 spectra. The mean plus two standard deviations of these 1,000 spectra were then taken as the statistical threshold to determine significance of modulation. It is important to note that the averaged white noise spectrum has greater power at low frequencies. This is due to the fact that the GWN data is band-limited, and this results in better representation of low frequencies than higher frequencies. This illustrates the importance of using a statistical threshold to determine significance, as band-limited random signals have a bias toward lower frequencies.

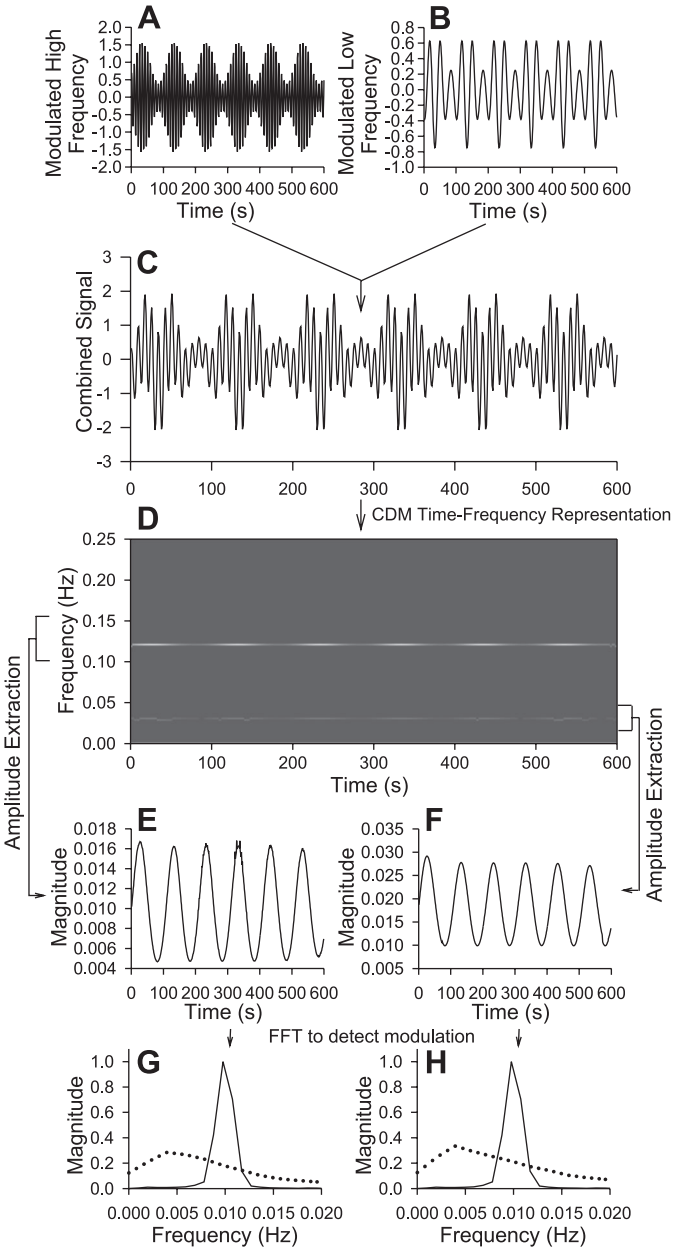

Fig. 2. Flowchart of the amplitude modulation detection algorithm using simulated data. *A* and *B*: 2 simulated signals amplitude modulated by a low-frequency (LF) component. *C*: summation of those 2 signals. This was done to simulate the conditions of the 2 renal autoregulatory mechanisms. *D*: complex demodulation (CDM) time frequency representation of the simulated data in *C*. *E* and *F*: average amplitude of the myogenic (MYO) and tubuloglomerular feedback (TGF) frequency range across time, at 0.01–0.03 and 0.02–0.05 Hz, respectively. *G* and *H*: fast Fourier transform (FFT) of the time traces from *E* and *F*, respectively, which shows the amplitude modulation peak. The dotted lines show the result from 1,000 random simulations of Gaussian white noise which underwent the same algorithm. This shows the statistical threshold for significant amplitude modulation.

Data Analysis

For the chirp forcing experiment, data were collected at 200 Hz, then low-pass filtered with a cutoff frequency of 0.1 Hz and down-sampled to 0.5 Hz. Finally, the data underwent linear trend removal and were normalized to 0 mean and unit variance.

All modulation analyses of data from conscious rats were performed on 10-min data segments. All data were filtered with a low-pass antialiasing filter followed by down-sampling to 1 Hz, which resulted in a total of 600 data points. This segment size was chosen because of the need to analyze only telemetric data sets that are free from substantial movement artifacts. The data were then normalized to 0 mean and unit variance to permit comparison between SHR and SDR. The CDM was employed with a fast Fourier transform segment size of 1,024 points (0 padding included), which yielded a resolution

of 0.000976 Hz. Because we collected telemetric data for 7 days, we were able to obtain 16–25 data sets of 10-min duration for each animal that were essentially free of motion artifacts. Analysis was performed on each segment, and the final results were averaged for each animal. Furthermore, the percentage of significant (motion-free) segments for each animal was recorded. For the acute data collected for 1 h in animals under anesthesia, the percentage of significant segments was not recorded.

Statistical analysis was done using the SigmaStat (Systat Software, San Jose, CA) software package. We used Student's *t*-test for two groups (e.g., SDR vs. SHR in the telemetric experiments), and one-way ANOVA for multiple groups (e.g., SDR vs. SHR in the anesthesia and telemetric experiments). The significance level was $P < 0.05$.

RESULTS

For the chirp data, all animals ($n = 5$) showed significant resonance oscillatory peaks in the vicinity of ~0.01 Hz, similar to the results shown in Fig. 1. The group average for the five animals is shown in Fig. 3. The solid line indicates the mean, while the dashed lines indicate the SD. The large solid line shows statistical significance above the 0 threshold, which is shown as a dotted line. The mean peak frequency was 9.0 ± 0.5 mHz for all animals.

Analysis of all of the data collected from conscious animals via telemetry and from isoflurane-anesthetized rats identified only significant AM via the modulation detection algorithm; FM was not significant. A representative time trace, along with its corresponding TFR, extracted AM signal, and its spectrum are shown in Fig. 4. The data shown in this figure are from a SDR telemetric experiment. We observed significant modulation frequency peaks at ~0.01 Hz, which were derived by extracting AM magnitude values from the MYO (*bottom left*) and TGF (*bottom right*) frequency bands. The assertion of significance is based on the fact that the peaks in Fig. 4, *E* and F, exceed the critical threshold calculated with band-limited GWN (see METHODS).

Figure 5 summarizes the results of the analyses of the telemetric data. The *left* and *right* panels show the detected AM results obtained from the MYO and TGF frequency bands, respectively. The *top* row shows the mean percentage of segments that exhibited significant AM. The *middle* row shows the average magnitude of the AM. The *bottom* row shows the average frequency associated with the detected AM. For both MYO and TGF frequency bands, the percentage of coupled segments are significantly higher (*$P < 0.05$) for SDR than SHR. Furthermore, we observed a greater AM effect on TGF than MYO (#$P < 0.05$) in SHR. As shown in the *middle* row, the magnitude of the AM effect on MYO and TGF was significantly greater (*$P < 0.05$) in SDR than SHR. The frequency of AM was found to be ~0.01 Hz in all cases.

For the acute data collected from animals under isoflurane anesthesia, the presence of the ~0.01-Hz autoregulation component was only evident in the form of AM in the MYO frequency band. Furthermore, the data from animals under inactin exhibited no significant AM or FM and are not shown. Figure 6 shows a comparison between acute experiments with isoflurane anesthetic and telemetric recordings in which there was clear AM of the MYO frequency band. Note that the two telemetric values are the same as in Fig. 5 and are included here to facilitate comparison. The results show that the AM magnitude in the MYO band for SDR telemetric recording was significantly different from the other conditions (*$P < 0.05$).

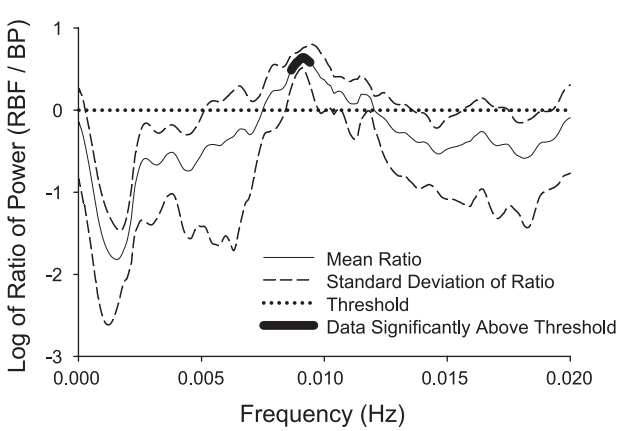

Fig. 3. Plot of the average of the ratio between the spectral power of the RBF vs. that of the BP, plotted in log scale ($n = 5$). The solid line shows the mean of the 5 animals, while the dashed line shows the SD. The dotted line shows the threshold of 0, where above this value indicates an active mechanism. The thick line in the mean ratio indicates statistically significant difference from the threshold line.

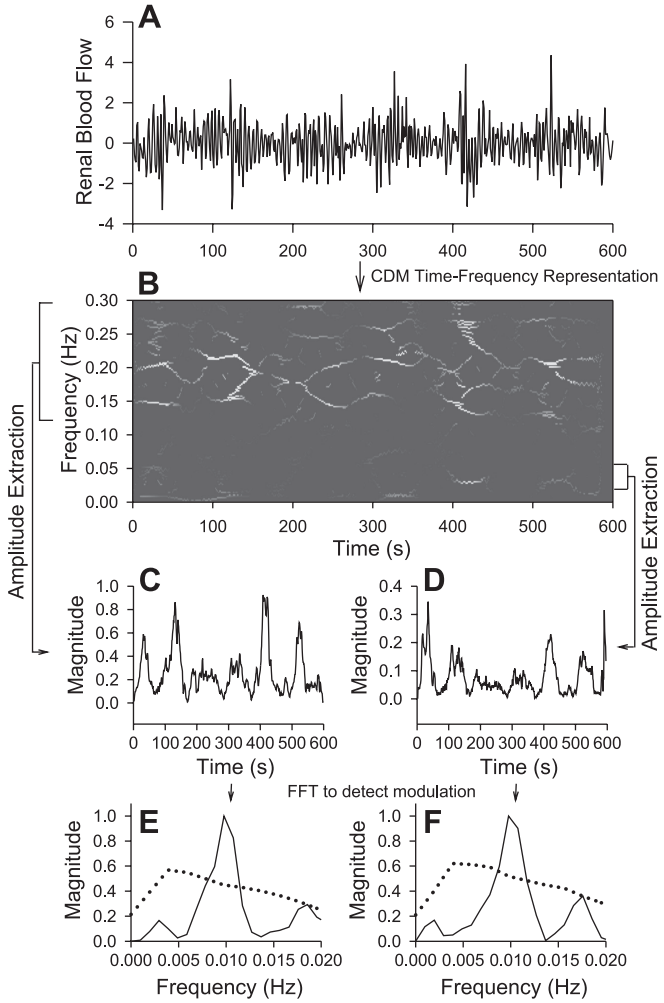

Fig. 4. Representative data set showing significant amplitude modulation. The particular data set shown is a recording from a telemetric experiment in a Sprague-Dawley rat (SDR). The calculation of the amplitude modulation is the same as that shown in Fig. 3.

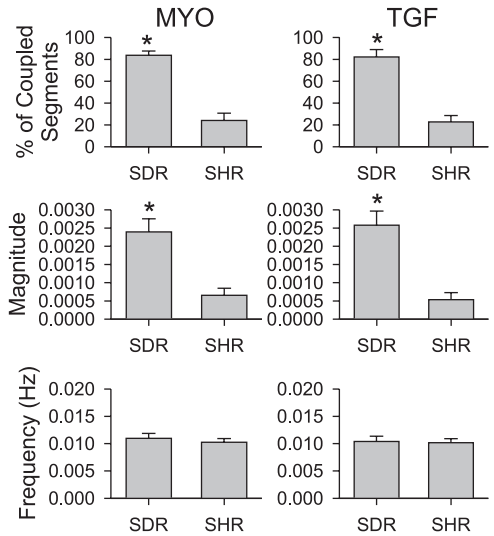

Fig. 5. Summary data for the telemetric experiments. Note that only the results for amplitude modulation are shown, as frequency modulation was not found to be significant. *Statistical significance between SDR and SHR ($P < 0.05$).

DISCUSSION

In this study, we detected the presence of the LF (~0.01 Hz) component in spontaneous blood flow recordings from both conscious and unconscious normotensive and hypertensive rats. Specifically, we found evidence of LF that modulates the amplitudes of the MYO and TGF oscillations, which is consistent with significant interactions of these autoregulatory systems with a LF component. Furthermore, we found a greater number of data segments that exhibit LF modulation of the TGF and MYO mechanisms in SDR than in SHR. In addition, the magnitude of the LF modulation of the MYO and TGF systems was greater in SDR than in SHR with telemetric recordings. With anesthetic agents, the magnitude of the LF modulation of the MYO and TGF components, compared with telemetric recordings, was suppressed by isoflurane and abolished by inactin. These observations were reinforced by separate experiments where a chirp forcing signal in BP was used to elicit resonant spectral peaks in the LF band. These results showed that there was, indeed, an active autoregulatory component in RBF in the LF range.

In previous studies, random BP forcings were used to examine the dynamic properties of renal autoregulation (16, 17). However, no LF components were observed in these studies. One possible explanation for this may be that in the past studies, the data segments were relatively short, which would limit the frequency resolution and, hence, the inability to resolve any LF component. In contrast, we analyzed much longer time records. Furthermore, our chirp signal forcing was specifically designed to elicit BP fluctuations in the LF range, whereas a random forcing does not guarantee that BP fluctuations in the LF range are well represented. Thus the chirp signal forcing is a more appropriate approach than random forcing to resolve LF components.

Work by Just and Arendshorst (12) identified a putative third renal autoregulatory mechanism with a response time and resonant frequency that coincides with the LF component we identified. Our approach to identification of the LF component is based on the hypothesis that if it does exists, it should interact with the MYO and TGF mechanisms. The support for our hypothesis stems from previous studies in which there is ample evidence of interactions between the MYO and TGF via experimental (21) and computational approaches (5, 20, 26). Furthermore, a study by Sosnovtseva et al. (25) found interactions between the MYO and TGF by searching for AM and FM phenomena between the two mechanisms using wavelet analysis. In the cardiovascular system, we found interactions between the sympathetic and parasympathetic nervous systems by obtaining evidence of AM and FM phenomena in heart rate variability signal (31). Thus the presence of AM and FM phenomena in biological signals is ubiquitous, and this has led us to look for the presence of the LF oscillation in renal hemodynamics by these means.

Identification of the third mechanism in the study of Just and Arendshorst (12) is based on time-domain measurements that examine the transition between steady states in renal blood flow elicited by step-changes in BP in rats under the influence of anesthesia (12). Our study differs from that of Just and Arendshorst in several ways. First, identification of the LF component is not based on inducing step-changes in BP but directly from the spontaneous recordings of RBF data. Thus we were able to use telemetric data from conscious rats for our analysis. The results show that anesthetics significantly suppress the interaction of the LF component. Therefore, the use of conscious recording is important in assessing the true dynamics of the putative LF autoregulatory component. Second, our method involves discrimination of the LF component in both time and frequency domains by searching for the presence of AM or FM dynamics, not just time-domain analysis as was employed by Just and Arendshorst. We have previously shown that accurate identification of renal autoregulatory dynamics such as interactions between the MYO and TGF requires time-varying approaches (20). In addition, the AM or FM phenomena are often difficult to resolve partly because they are time-varying. Thus our successful identification of AM was predicated on the use of one of the highest resolution time-frequency spectral techniques available (28). We have shown that our CDM time-frequency method performs better than the wavelet approach, and in some cases, it outperforms the parametric time-varying autoregressive model-based spectrum (28).

It is important to note that the third mechanism of renal autoregulation proposed by Just and Arendshorst (12) and the LF component detected by our two analytic approaches in the

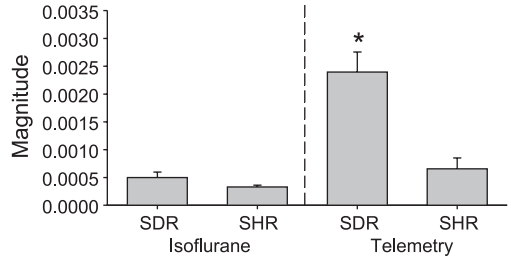

Fig. 6. Summary data from the acute experiments. Results from the telemetric experiments are also shown, to facilitate comparison. Note that only data from MYO amplitude modulation is shown, as TGF did not show significant modulation in acute experiments. Furthermore, the results from inactin-anesthetized animals are not shown as they were also not significant. *Data sets significantly different from all others.

present study operate on similar time scales. The use of a chirp signal as BP forcing resulted in a significant resonant gain peak centered at 0.01 Hz when we calculated the ratio between RBF and BP spectra. The gain magnitude values decreasing below 0 dB in Fig. 3 at frequencies lower than 0.01 Hz is a hallmark of dynamic autoregulation. Previous time-invariant (4, 8) and time-varying (6) transfer function analyses show such characteristics at the MYO and TGF frequency ranges, thereby leading to our assertion that they are autoregulatory mechanisms. The LF component detected via the AM phenomenon being related to the possible third autoregulatory mechanism is less obvious than results from the chirp signal forcing experiment. However, having found evidence of interactions between the LF component and both TGF and MYO, and because this LF component is identical to the frequency of the resonant gain peak, we can surmise that 0.01-Hz detection via the AM is also related to the autoregulatory dynamics. Although not shown, it should be noted that we also observed significant interactions between the MYO and TGF in the form of the latter's amplitude and frequency modulating the former. This is not surprising, as previous studies have shown evidence of both AM and FM of the MYO by the TGF (27).

The results of the telemetric data show that the magnitude of AM is reduced in the SHR compared with SDR. This finding is consistent with previous studies. Sosnovtseva et al. (27) showed that synchronization between the two traditional modes of renal autoregulation is reduced in SHR. In our own laboratory, we also observed a decrease in coupling between the MYO and TGF mechanisms in SHR using a bispectrum approach (22). However, it is important to note that where the past studies showed evidence of frequency modulation, our study only detected a significant AM. This may suggest that the slow modulation mechanism interacts with the two established modes of renal autoregulation differently.

The presence of FM of the LF on either TGF or MYO was not detected in this work. The presence of FM was searched by tracking frequencies associated with the significant amplitudes in the MYO and TGF frequency bands across time. As shown in Fig. 4, searching for the presence of FM is difficult in the MYO frequency band because frequencies tend to vacillate over time. To circumvent a subjective selection of which frequency to select at each time point, we used a weighted frequency average technique as described in METHODS. While we did not detect the LF component frequency modulating either the MYO or TGF, we did find evidence of FM of the MYO by the TGF. This is in agreement with a previously reported study which also found such FM phenomenon using a double-wavelet approach (25).

Figure 6 shows that the use of isoflurane anesthetic reduced the magnitude of the LF modulation in the MYO frequency range. In general, this is not surprising, as anesthetics tend to suppress physiological dynamics. Of more importance is the difference between isoflurane and inactin, where the presence of the LF modulation is abolished with inactin.

The presence of AM and FM of the TGF and MYO by a slow component was recently reported by Pavlov et al. (18). The present study differs from this previous study in three ways. First, our study employed both conscious and isoflurane-anesthetized animals vs. halothane anesthesia in the previous study. Halothane is known to simplify renal blood flow dynamics (7). Second, we measured total renal blood flow, thus averaging over ~1,600 cortical radial arteries vs. a single cortical radial artery in the previous study. Third, the significance of detection of AM and FM phenomena was tested against white noise threshold values whereas the previous study did not employ such statistical measurement.

Previous studies have shown that ANG II is involved in the modulation of both the TGF (19) and the MYO (15). ANG II also mediates the low BP resetting of renal autoregulation (7, 24). Furthermore, low BP has been shown to induce renal vasoconstriction on a similar time scale as the LF component (7). Therefore, one could not exclude a possible role of the renin-angiotensin system in the LF component.

In summary, the present study used two novel approaches to detect the presence of a LF component in RBF signals: *1*) chirp signal forcing and *2*) a signal-processing approach in which we specifically searched for the presence of the LF component by quantifying its effect to modulate the amplitude of oscillations of the TGF and MYO mechanisms. Our results suggest that one discriminator between the SHR and SDR is the lower magnitude of AM with the latter. We see that isoflurane diminished the magnitude of the LF component whereas inactin abolished our detection of either the AM or FM phenomenon of the LF component. Our transfer function analysis of chirp signal data yielded a resonant peak centered at 0.01 Hz that is greater than 0 dB, whereas at lower frequencies the transfer function gain diminished to less than 0 dB, providing direct evidence of the LF being one of the autoregulatory mechanisms. Furthermore, our detection via the AM approach of interactions between the LF component and both TGF and MYO, with the LF component having an identical frequency to that of the resonant gain peak, provides more evidence that 0.01-Hz oscillations may represent the third autoregulatory mechanism.

REFERENCES

1. **Bidani AK, Griffin KA.** Long-term renal consequences of hypertension for normal and diseased kidneys. *Curr Opin Nephrol Hypertens* 11: 73–80, 2002.
2. **Bidani AK, Griffin KA.** Pathophysiology of hypertensive renal damage: implications for therapy. *Hypertension* 44: 595–601, 2004.
3. **Chen YM, Yip KP, Marsh DJ, Holstein-Rathlou NH.** Magnitude of TGF-initiated nephron-nephron interactions is increased in SHR. *Am J Physiol Renal Fluid Electrolyte Physiol* 269: F198–F204, 1995.
4. **Chon KH, Chen YM, Holstein-Rathlou NH, Marsh DJ, Marmarelis VZ.** On the efficacy of linear system analysis of renal autoregulation in rats. *IEEE Trans Biomed Eng* 40: 8–20, 1993.
5. **Chon KH, Chen YM, Marmarelis VZ, Marsh DJ, Holstein-Rathlou NH.** Detection of interactions between myogenic and TGF mechanisms using nonlinear analysis. *Am J Physiol Renal Fluid Electrolyte Physiol* 267: F160–F173, 1994.
6. **Chon KH, Zhong Y, Moore LC, Holstein-Rathlou NH, Cupples WA.** Analysis of nonstationarity in renal autoregulation mechanisms using time-varying transfer and coherence functions. *Am J Physiol Regul Integr Comp Physiol* 295: R821–R828, 2008.
7. **Cupples WA.** Angiotensin II conditions the slow component of autoregulation of renal blood flow. *Am J Physiol Renal Fluid Electrolyte Physiol* 264: F515–F522, 1993.
8. **Cupples WA, Braam B.** Assessment of renal autoregulation. *Am J Physiol Renal Physiol* 292: F1105–F1123, 2007.
9. **Daniels FH, Arendshorst WJ.** Tubuloglomerular feedback kinetics in spontaneously hypertensive and Wistar-Kyoto rats. *Am J Physiol Renal Fluid Electrolyte Physiol* 259: F529–F534, 1990.
10. **Holstein-Rathlou NH, Leyssac PP.** TGF-mediated oscillations in the proximal intratubular pressure: differences between spontaneously hypertensive rats and Wistar-Kyoto rats. *Acta Physiol Scand* 126: 333–339, 1986.

11. **Holstein-Rathlou NH, Marsh DJ.** Renal blood flow regulation and arterial pressure fluctuations: a case study in nonlinear dynamics. *Physiol Rev* 74: 637–681, 1994.
12. **Just A, Arendshorst WJ.** Dynamics and contribution of mechanisms mediating renal blood flow autoregulation. *Am J Physiol Regul Integr Comp Physiol* 285: R619–R631, 2003.
13. **Just A, Arendshorst WJ.** Nitric oxide blunts myogenic autoregulation in rat renal but not skeletal muscle circulation via tubuloglomerular feedback. *J Physiol* 569: 959–974, 2005.
14. **Just A, Ehmke H, Toktomambetova L, Kirchheim HR.** Dynamic characteristics and underlying mechanisms of renal blood flow autoregulation in the conscious dog. *Am J Physiol Renal Physiol* 280: F1062–F1071, 2001.
15. **Kirton CA, Loutzenhiser R.** Alterations in basal protein kinase C activity modulate renal afferent arteriolar myogenic reactivity. *Am J Physiol Heart Circ Physiol* 275: H467–H475, 1998.
16. **Marmarelis VZ, Chon KH, Chen YM, Marsh DJ, Holstein-Rathlou NH.** Nonlinear analysis of renal autoregulation under broadband forcing conditions. *Ann Biomed Eng* 21: 591–603, 1993.
17. **Marmarelis VZ, Chon KH, Holstein-Rathlou NH, Marsh DJ.** Nonlinear analysis of renal autoregulation in rats using principal dynamic modes. *Ann Biomed Eng* 27: 23–31, 1999.
18. **Pavlov AN, Sosnovtseva OV, Pavlova ON, Mosekilde E, Holstein-Rathlou NH.** Characterizing multimode interaction in renal autoregulation. *Physiol Meas* 29: 945–958, 2008.
19. **Ploth DW, Rudulph J, LaGrange R, Navar LG.** Tubuloglomerular feedback and single nephron function after converting enzyme inhibition in the rat. *J Clin Invest* 64: 1325–1335, 1979.
20. **Raghavan R, Chen X, Yip KP, Marsh DJ, Chon KH.** Interactions between TGF-dependent and myogenic oscillations in tubular pressure and whole kidney blood flow in both SDR and SHR. *Am J Physiol Renal Physiol* 290: F720–F732, 2006.
21. **Schnermann J, Briggs JP.** Interaction between loop of Henle flow and arterial pressure as determinants of glomerular pressure. *Am J Physiol Renal Fluid Electrolyte Physiol* 256: F421–F429, 1989.
22. **Siu KL, Ahn JM, Ju K, Lee M, Shin K, Chon KH.** Statistical approach to quantify the presence of phase coupling using the bispectrum. *IEEE Trans Biomed Eng* 55: 1512–1520, 2008.
23. **Skinner SL, McCubbin JW, Page IH.** Angiotensin in blood and lymph following reduction in renal arterial perfusion pressure in dogs. *Circ Res* 13: 336–345, 1963.
24. **Sorensen CM, Leyssac PP, Skøtt O, Holstein-Rathlou NH.** Role of the renin-angiotensin system in regulation and autoregulation of renal blood flow. *Am J Physiol Regul Integr Comp Physiol* 279: R1017–R1024, 2000.
25. **Sosnovtseva OV, Pavlov AN, Mosekilde E, Holstein-Rathlou NH, Marsh DJ.** Double-wavelet approach to study frequency and amplitude modulation in renal autoregulation. *Phys Rev E Stat Nonlin Soft Matter Phys* 70: 031915, 2004.
26. **Sosnovtseva OV, Pavlov AN, Mosekilde E, Holstein-Rathlou NH, Marsh DJ.** Double-wavelet approach to studying the modulation properties of nonstationary multimode dynamics. *Physiol Meas* 26: 351–362, 2005.
27. **Sosnovtseva OV, Pavlov AN, Mosekilde E, Yip KP, Holstein-Rathlou NH, Marsh DJ.** Synchronization among mechanisms of renal autoregulation is reduced in hypertensive rats. *Am J Physiol Renal Physiol* 293: F1545–F1555, 2007.
28. **Wang H, Siu K, Ju K, Chon KH.** A high resolution approach to estimating time-frequency spectra and their amplitudes. *Ann Biomed Eng* 34: 326–338, 2006.
29. **Wang X, Cupples WA.** Interaction between nitric oxide and renal myogenic autoregulation in normotensive and hypertensive rats. *Can J Physiol Pharmacol* 79: 238–245, 2001.
30. **Wang X, Loutzenhiser RD, Cupples WA.** Frequency modulation of renal myogenic autoregulation by perfusion pressure. *Am J Physiol Regul Integr Comp Physiol* 293: R1199–R1204, 2007.
31. **Zhong Y, Bai Y, Yang B, Ju K, Shin K, Lee M, Jan KM, Chon KH.** Autonomic nervous nonlinear interactions lead to frequency modulation between low- and high-frequency bands of the heart rate variability spectrum. *Am J Physiol Regul Integr Comp Physiol* 293: R1961–R1968, 2007.